Journal of The Korean Astronomical Society
46: 161 ∼ 172, 2013 August
©2013 The Korean Astronomical Society. All Rights Reserved.
http://dx.doi.org/10.5303/JKAS.2013.46.4.161
ISSN:1225-4614
http://jkas.kas.org

FOCAL REDUCER FOR CQUEAN (Camera for QUasars in EArly uNiverse)

Juhee Lim[1], Seunghyuk Chang[2], Soojong Pak[1], Youngju Kim[3], Won-Kee Park[4,5], and Myungshin Im[5]
[1] School of Space Research, Kyung Hee University, Yongin, Gyeonggi 446-701, Korea
E-mail : juheelim@khu.ac.kr, soojong@khu.ac.kr
[2] Samsung Electronics Co., Ltd., Suwon, Gyeonggi 443-370, Korea
[3] Yunam Optics Inc., Icheon, Gyeonggi 467-811, Korea
[4] Korea Astronomy and Space Science Institute, Daejeon 305-348, Korea
[5] CEOU/Departmet of Physics and Astronomy, Seoul National University, Seoul 151-741, Korea
(Received March 17, 2013; Revised July 16, 2013; Accepted July 29, 2013)

ABSTRACT

A focal reducer is developed for CQUEAN (Camera for QUasars in EArly uNiverse), which is a CCD imaging system on the 2.1 m Otto Struve telescope at the McDonald observatory. It allows CQUEAN to secure a wider field of view by reducing the effective focal length by a factor of three. The optical point spread function without seeing effects is designed to be within one pixel (0.283″) over the field of view of $4.82' \times 4.82'$ in optimum wavelength ranges of $0.8 - 1.1$ μm. In this paper, we describe and discuss the characteristics of optical design, the lens and barrel fabrications and the alignment processes. The observation results show that the image quality of the focal reducer confirms the expectations from the design.

Key words : Instrumentation — optical system, optics, focal reducer: Galaxy — high-redshift: Quasars — general

1. INTRODUCTION

The use of CCD is dominant in astronomical observation these days. The advances in semiconductor technology increase the quantum efficiency and reduce readout noise. As a result, recent CCDs with small pixels often provide equal or even greater performance compared to the CCDs with large pixels of the past. We can use an image sensor of smaller format while maintaining sensitivity. However, a telescope with shorter focal length is also required to obtain an adequate field of view with smaller sensor size.

A focal reducer is an auxiliary optical device that reduces the focal length of a telescope. It also corrects the off-axis aberrations of the telescope and enlarges the usable field of view. There are two types of focal reducers - one with an intermediate image and the one without it (Wilson 1996). The former consists of a collimator and a camera in general, and is suitable for a spectrograph as the collimator produces parallel beams. For the latter, the optical configuration is simple, but correcting abberation mechanism is more complex.

We developed a focal reducer for CQUEAN (Camera for QUasars in EArly uNiverse: Park et al. 2012; Kim et al. 2011), which is an optical CCD camera optimized for observations of red objects including high redshift quasar candidates ($z > 5$; e.g., Choi et al. 2012), transient objects such as Gamma Ray Bursts and supernovae (Thöne et al. 2011; Lee et al. 2010), and young stellar objects (Green et al. 2013). The focal reducer was specifically designed to be used with the 2.1 m Otto Struve telescope of McDonald observatory in Texas, US. The overall description of the CQUEAN system including the basic optical design is in Park et al. (2012). In this paper, we present and discuss the detailed design and fabrication of the focal reducer lenses, the camera barrel design, and the optical alignment test and the optical performance of the astronomical observations.

Corresponding Author: S. Pak

2. OPTICAL DESIGN

2.1 Design Requirements

We use a backside-illuminated deep-depletion CCD camera (iKon-M DU934 BR-DD, Andor Technology) for the CQUEAN system. The CCD format is 1024×1024 with 13 μm pixel size. The pixel scale of the CCD is 0.094″/pixel at the Cassegrain focus of the McDonald 2.1 m telescope, which is an f/13.65 classical Cassegrain system. The FWHM of a typical seeing at the McDonald Observatory is around 1.2″. Thus with CCD pixel sizes of 12 - 30 μm, the seeing disk is inefficiently oversampled (Opal & Booth 1990). The observed point spread function (PSF) would take more than 10 pixels on the science CCD. The small pixel scale also limits the CCD field of view (FOV) only to $1.6' \times 1.6'$.

We designed the focal reducer to reduce the effective focal length by a factor of three. As described in

Table 1.
Optical specifications of the McDonald 2.1 m telescope and the CQUEAN system

Parameter	Cassegrain focus	with focal reducer
D_{tel}(aperture diameter)	2.083 m	
Telescope effective focal length	28.425 m	9.475 m
CCD pixel size	13×13 μm	
CCD format	1024×1024 pixels	
Pixel scale	$0.094''$/pixel	$0.283''$/pixel
Field of view[a]	$1.6' \times 1.6'$	$4.83' \times 4.83'$

[a] The available FOV with the focal reducer is limited within the radius of $2.4'$.

Table 1, the pixel scale becomes $0.283''$/pixel so that the FWHM of a stellar profile can be covered about 4 pixels under the typical seeing condition (see also the basic optical design in Park et al. 2012).

2.2 Optical Layout

We designed the optical system using ZEMAX. Fig. 1 and Table 2 show the optical layout and a detailed description of the optical system, respectively (Park et al. 2012). The focal reducer consists of four spherical lenses (one doublet and two singlet lenses) and converts the f/13.6 telescope to the f/4.6 system. All lens surfaces are spherical, and the optical glasses were manufactured by Schott Glass Technologies, Inc.

The CCD camera window is made of fused silica with a thickness of 1.5 mm. The filters were made by Asahi Spectra, Inc. The composite thickness of the filters is $5 - 8$ mm, composed of ionically colored glass, e.g., Schott BB39 or colloidally colored glass, e.g., GG400, OG550, RG610, and RG695, and fused silica. Even the refractive indexes of the ionically colored glass and the colloidally color glass ($n = 1.51 - 1.55$) are little higher than that of the fused silica ($n = 1.45 - 1.46$), we approximate that the filters are composed of silica with thickness of 5 mm. The total track length from the front surface of the Lens 1 to the CCD is 132.06 mm considering the focal plane shift caused by different refractive indexes of the filter and the CCD window.

In the optimization processes, we did not seriously consider chromatic aberration and image qualities on the 4 corners of the CCD field of view, in order to reduce the manufacturing complexity. The wavelength bands of our scientific interest are limited to $0.7 - 1.1$ μm, and we would not make a large field of view mosaic image. As a result, the second-order term of longitudinal chromatic aberration has not been removed. Linear dependence of the spherical aberration on wavelength has not been eliminated, either. However, spherical aberration at the wavelength of 1.0 μm, for both the third and fifth order terms, was kept almost zero.

2.3 Optical Performance

We evaluated the performances of the optical design in the forms of spot size, modulation transfer function (MTF) and Seidel aberration coefficients. The considered wavelength range is from 0.8 μm to 1.1 μm and the considered field of view is within the radius of $2.4'$.

A geometrical spot diameter on the detector plane presents the whole regions of the rays from a point source at infinity. This diameter, however, can be misleading in case of inhomogeneous distribution, e.g., by coma aberration. Hence, instead of geometrical spot diameter we use RMS (root-mean-square) spot diameter to evaluate the quality of the optics. This diameter is equivalent to the image area where approximately 70% of incident rays is concentrated. Fig. 2 shows the spot diagrams with and without focal reducer at the image plane, created using ZEMAX. Without the focal reducer, the spot diagram shows serious coma aberration at the edge region of the image because the 2.1 m Otto Struve Telescope is a classical Cassegrain type. The RMS spot diameter on the $2.4'$ offset position from the optical axis is 26.9 μm which corresponds to two pixels. The focal reducer was designed to correct coma aberration and astigmatism by running optimization processes of a ray tracing program. The corrected RMS spot diameter at the $2.4'$ field position is 8.6 μm, which is much smaller than a single pixel.

MTF, another indicator of the performance, is a direct measure of the optical quality of non-point source image (Smith 2005). The highest spatial frequency of interest in our system is determined by the CCD pixel size (13 μm) and Nyquist sampling.

$$f = \frac{1}{2} \times \frac{1}{13\mu m} = 38.5\ cycles/mm \qquad (1)$$

As we can see in Fig. 3, the MTF values are higher than 68% for the entire field of view when the focal reducer is used.

Fig. 4 shows various Seidel aberration coefficients of the optical system including the telescope, the focal reducer, the filter, and the CCD window. They were calculated at the wavelength of 1.0 μm. The aberrations on the primary and secondary mirrors of the telescope show significant spherical and coma aberrations, but those are cancelled out by each other. In the focal reducer, distortion appears to be particularly large for each lens. However, as they are cancelled out by other

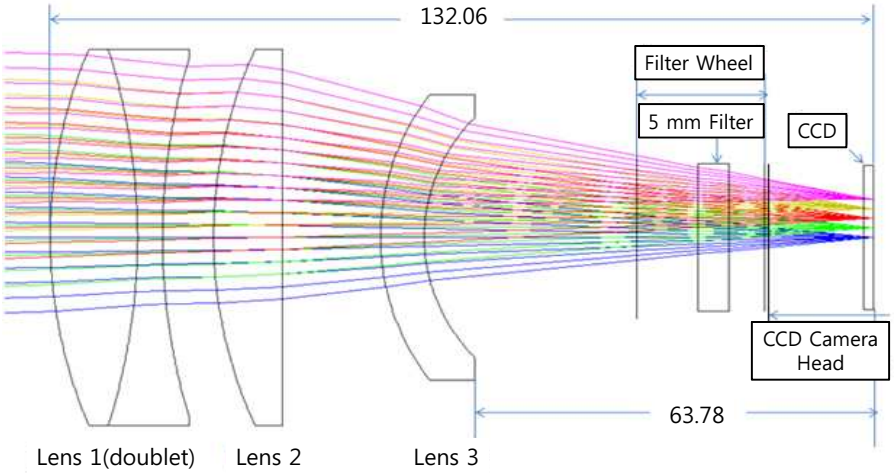

Fig. 1.— Optical configuration of the focal reducer (Park et al. 2012).

Table 2.
Optical system prescriptions from the telescope to the CCD (Units are millimeters.)

Surface	Comments	Radius of curvature	Thickness	Glass material	Semi-diameter	Conic constant
object		infinity	infinity		infinity	0.00
1		infinity	6079.00		1045.72	0.00
2 (stop)	Telescope primary	-16239.000	-6079.00	MIRROR	1041.50	-0.98
3	Telescope secondary	-5715.000	6079.00	MIRROR	266.27	-2.98
4		infinity	700.10		56.34	0.00
5	Lens 1	91.188	14.00	NBAF10	33.00	0.00
6	(doublet)	-118.153	4.00	N-SF66	33.00	0.00
7		118.153	8.20		31.50	0.00
8	Lens 2	84.927	11.00	SF57	33.00	0.00
9		infinity	15.80		33.00	0.00
10	Lens 3	43.774	7.00	N-FK5	25.00	0.00
11		31.344	43.88		21.00	0.00
12	Filter	infinity	5.00	SILICA	12.90	0.00
13		infinity	21.68		12.90	0.00
14	CCD window	infinity	1.50	SILICA	12.70	0.00
Image		infinity			6.65	0.00

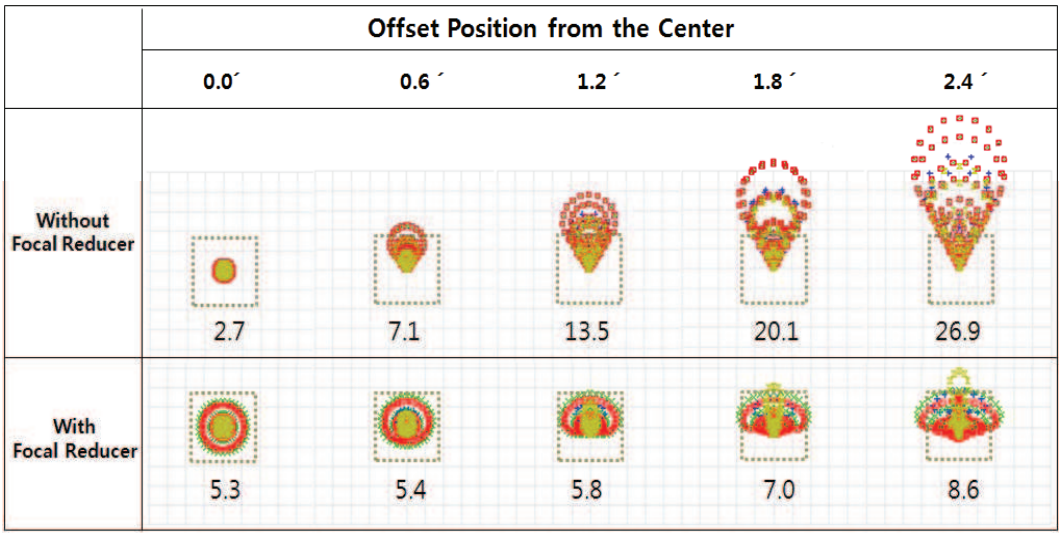

Fig. 2.— Geometrical spot diagrams against the field angle without (upper panel) and with (lower panel) our focal reducer at the best composite focus. Plotted wavelengths are 0.8 μm, 0.9 μm, 1.0 μm, and 1.1 μm in yellow, red, green, and blue colors, respectively. The green box shows the size of a pixel (13 $\times$ 13 μm). The numbers under the green boxes are the RMS spot diameters in units of μm.

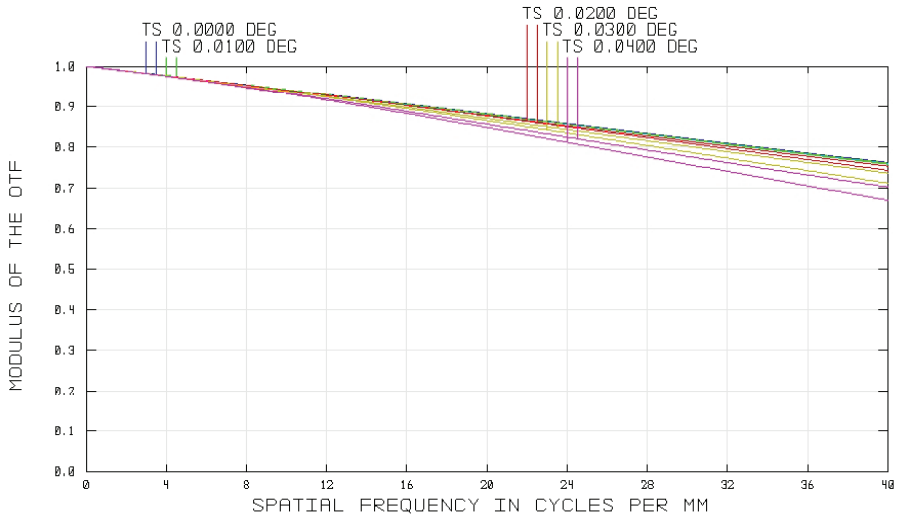

Fig. 3.— Modulation transfer function of the telesocpe with the focal reducer.

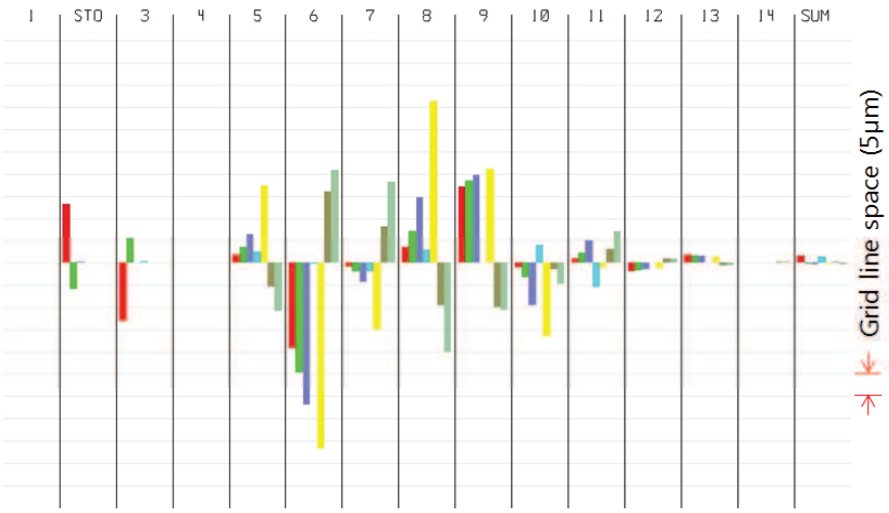

Fig. 4.— Seidel aberration coefficients. Plotted coefficients are spherical aberration (red), coma (green), astigmatism (blue), field curvature (pale blue), distortion (yellow), longitudinal color (dark gray), and transverse color (light gray). The maximum aberration in the scale bar is 50 μm and the grid lines are spaced by 5 μm. The wavelength used for the calculation is 1.0 μm. The vertical grids indicate the surfaces of the optical components (see Table 2).

lens elements, the final result at the SUM column in the figure is close to zero. Likewise, the results of all the aberrations are minimized at the image plane.

2.4 Sensitivity Analysis and Alignment Tolerance

Performance degradation of an optical system usually results from tilt, decenter, or despace of its components and/or from their surface deformations. A sensitivity analysis investigates how much the optical system is perturbed by those individual parameters (Schroeder 2000). It is important to create a design that is not too sensitive to construction parameters.

In the sensitivity analysis, we need criteria of optical performance within which the perturbations of optical parameters are allowed. The final image quality of the system from the atmosphere through the CCD can be approximated as a quadrature sum of the seeing and the image blur by the optical system. As a criterion to control the performance of the focal reducer, we limit the total image quality not to exceed 110% of the seeing size. This means that the spot size of the optical system should be smaller than 11.054 μm RMS.

Table 3 shows the results from the sensitivity analysis where a sensitivity parameter is perturbed within the image quality range ($<$ 11.054 μm RMS) to seek the maximum allowable value of the tolerance, while other parameters are fixed except the position of the telescope secondary with which we can compensate the perturbed effective focal length. We assumed that the doublet has no airspace and it does not have any tolerance between the inner two surfaces. The maximum spot sizes mean the largest values resulting from perturbations in all axes and fields, while spot sizes of each field represent the spot size from the perturbation in zero and positive object fields only as an example. It can be allowed because tilt and decenter of this system are symmetric with respect to the axis, and despace is along the z-axis.

Compared to the other parts, despace of Lens 3 is much more sensitive. However, manufacture is still possible considering our manufacturing tolerance range for the lens barrel. Firstly, we consider the material of lens barrel to analyze the tolerance range. In general, aluminium 6061 has higher self-strain due to the higher coefficient of thermal expansion than glass type material. Also, aluminium surface is not polished with fine sand particles as for glasses, but carved in cutting machines. Therefore, aluminium part has relatively large tolerance ($\pm$ 10 μm) in manufacturing. Secondly, in the process of making a lens barrel, shape tolerance in concentricity is considered to be the more important than dimensional tolerances. The lens barrel is designed to achieve 0.5 μm for the concentricity tolerance because decenters of all lenses and other parts are constrained by the mounting base. Thirdly, outer diameters of spacers, which contact with the mount, are usually processed with tolerances of $\sim$ 30 μm from the original dimensions. Inner diameter tolerance is $\pm$ 10 μm, and the same for thickness tolerance. Finally, retainers have tolerance level of general purpose fabrication ($\pm$ 50 μm).

In practice, misalignment error of each optical element contributes to the overall degradation of system image quality combined with other errors. Assuming that all the error components are independent with

Table 3.
Result of the sensitivity analysis. The wavelength used for the calculation is 1.0 μm. (Unit of tilt is degree, and decenter and despace are shown in mm)

Parameter	Lens	Max. tolerance	RMS Spot size of each field (μm)					Max. RMS
		value(+/-)	0 deg	0.01 deg	0.02 deg	0.03 deg	0.04 deg	spot size (μm)
Tilt	Lens1	0.639	4.960	5.800	7.197	8.770	10.562	11.031
	Lens2	0.393	5.458	5.546	6.814	8.804	10.584	11.021
	Lens3	1.008	2.517	2.697	4.669	7.615	11.036	11.036
Decenter	Lens1	0.258	3.235	4.433	6.035	8.009	10.845	11.030
	Lens2	0.194	3.096	2.860	4.395	7.194	10.780	11.030
	Lens3	0.790	2.438	3.928	5.806	7.981	10.841	11.032
Despace	Lens1	0.945	10.567	10.560	10.556	10.640	11.041	11.041
	Lens2	3.060	9.013	9.078	9.315	9.865	11.044	11.044
	Lens3	0.069	10.077	10.099	10.184	10.410	11.014	11.014

each other, we can combine the errors into a quadrature sum. To build an error budget in Table 4, we apply the perturbation of maximum alignment tolerances, which are provided by the manufacturer (Green Optics Co.), to the parameters and calculate the resulting increments in spot sizes (the last column in Table 4). Typical tolerance of spacer and the lens barrel is 30 μm. Tilt tolerances can be calculated from this information.

As a result, quadruture sum of individual contributions to the image degradation is calculated to be 5.028 μm, which enlarges the RMS spot size from 4.312 μm to 9.340 μm. This means that the image degradation by the probable alignment error is less than the performance criteria for the focal reducer, 11.054 μm RMS, described previously.

Thus we conclude that our focal reducer design is quite robust against alignment errors and should not degrade the image quality of the CQUEAN system further from the seeing condition. As seen in the sensitivity calculations, despace of Lens 3 is most sensitive and thus makes the greatest contribution to the error budget. Therefore, further improvement of optical performance is possible by controlling the tolerance of this part.

3. LENS BARREL

We carried out mechanical design of the telescope interface including the lens barrel of the focal reducer. AutoCAD 2009 was used for modelling the optomechanical systems and graphically portraying computational results. The barrel consists of two housing pieces (mounts), one spacer, three retainers for securing lenses into their mounts, and a cover for protecting the first lens (see Fig. 5). We designed the back focal length to be adjusted within a range of $\pm$3 mm in order to compensate the uncertain filter material and thickness, the telescope secondary adjustment is enough to correct the effective focal length. The spacer and retainers contact lenses on their polished surfaces leaving radial clearances around the rims.

The barrel is designed to fit closely with the lenses. A good quality lens is made with a +0.000/-0.001 inch tolerance for diameter and the tolerance for the inner diameter of a barrel is +0.001/-0.000 inch so that there is as large clearance as 0.002 inch between the two diameters (Smith 2000). Large diameter optics like in our case is usually specified with somewhat looser tolerances. We confirmed that each spacer and retainer were made within the required tolerances by actual measurements of dimensions.

Fig. 6 shows an inside view of the lens barrel including its threaded baffle. Stray light from outside of the FOV could be reflected from the inner walls of the housing and degrade performance of the system. Baffle vanes are typically used to reduce intensity of light that is reflected from the walls. A threaded baffle is another method to reduce the light in an inexpensive and highly effective way. The tops of threads should not be completely sharp. Flat-top threads are better to keep the stray light out of the optical path to the detector. Angle of threads also influences the performance of scattering suppression. To make the threads angle blunt, we set the distance between the neighboring tops is longer than 0.25 mm. In general, a reasonable machining limit for sharpness of a threads baffle is in the range of 0.1 - 0.25 mm (Smith 1998). A baffle cap is attached to the front of the focal reducer for the additional shielding of the light coming from sources outside the FOV as shown in Fig. 5.

4. ASSEMBLY AND ALIGNMENT

In the assembly process, tilt of each lens at each step was measured using a centering telescope (see Fig. 7). The centering telescope is a type of focometer alignment error-sensing instrument. It measures performance of lenses or a complete optical system as the position and orientation of an optical component is

Table 4.
Alignment tolerances and error budget (Unit of tilt is degree, and decenter and despace are shown in mm)

Parameter	Lens	Maximum tolerance value	Maximum RMS spot size (μm)	Max-original spot size (μm)
Original spot size		-	4.312	0.000
Tilt	Lens1	0.104	4.636	0.324
	Lens2	0.087	4.897	0.585
	Lens3	0.115	4.549	0.237
Decenter	Lens1	0.080	5.334	1.022
	Lens2	0.080	6.066	1.754
	Lens3	0.080	4.575	0.263
Despace	Lens1	0.060	4.564	0.252
	Lens2	0.050	4.371	0.059
	Lens3	0.050	8.842	4.530

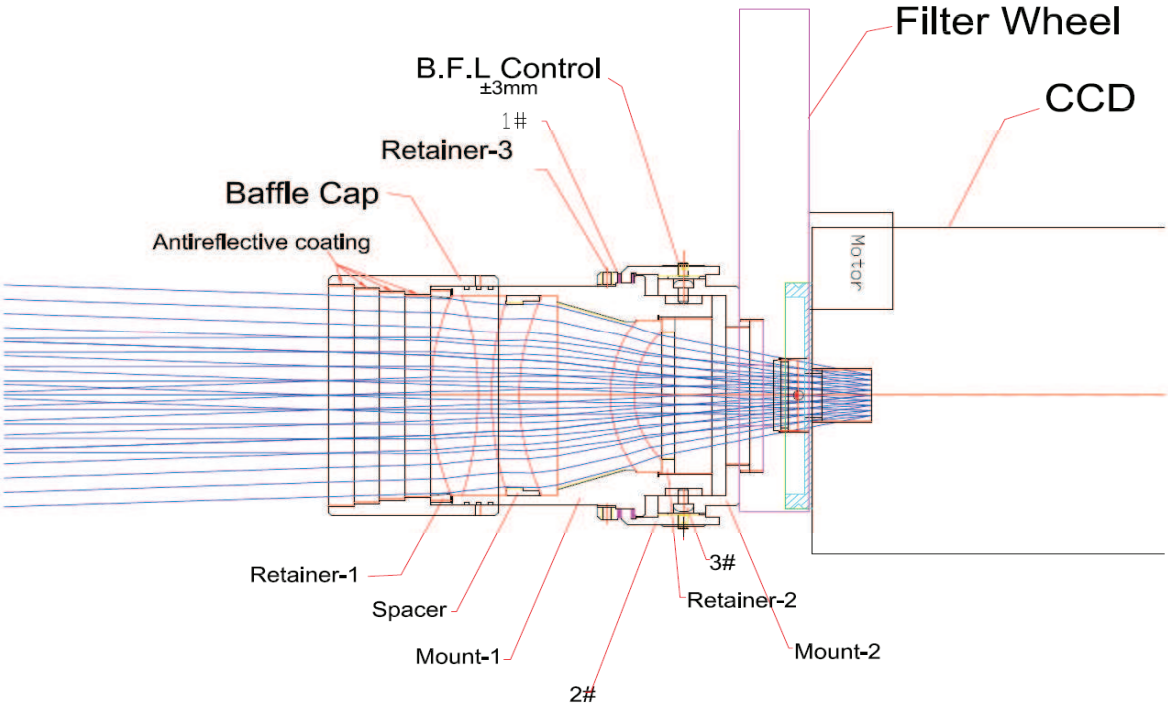

Fig. 5.— Lens barrel design of the focal reducer. The filter wheel and CCD camera module are attached to the focal reducer barrel. The surface of baffle cap as well as all barrel components are anodized with black color.

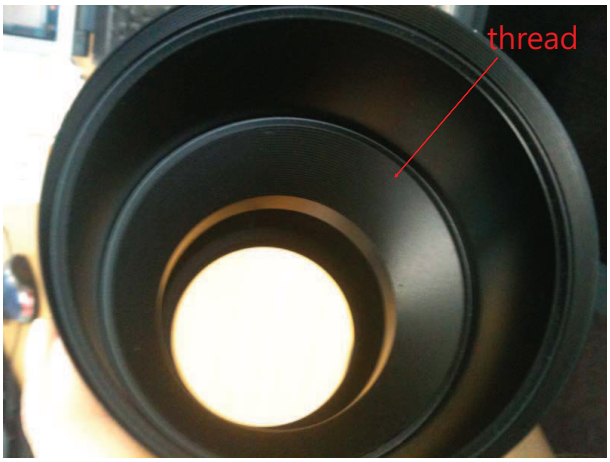

Fig. 6.— Completed lens barrel. Threads are applied inside the barrel for blocking the stray light reflected from the inner wall.

adjusted during assembly. If a perfectly centered and edged lens is rim-mounted in a perfect cell, the image of a distant axial object point will be centered on the axis. Axial location of the lens is usually controlled by forces applied to the spherical surfaces by clamping the lens between retainers, spacers, etc.

The focal reducer is assembled in the following procedure. Firstly, the focal reducer barrel is placed on the testing plate of the centering telescope to check its balance by rotating the plate. Initial placement of the barrel is measured by robot-arm probes. We set up the initial placement error to be within a range of $\pm$ 10 μm. The lens assembly was started from Lens 3, and initial position of the reflector in the centering telescope was predicted by ZEMAX. This process was repeated while stacking Lens 2 and Lens 1 in sequence. We assembled the lenses one by one while measuring effective tilt angle of the lens set stacked up to that step of assembly process.

After installing each lens, we measured the focal length and the tilt angle. The tilt angle was calculated from the radius of image rotation at the focal position caused by rotation of the testing lens set on the base plate. As seen in Table 5, tilt by the combination of Lenses 3 and 2 is larger than tilt by Lens 3 alone. But it decreases when Lens 1 is added because of a compensation effect. As a result, effective tilt of the entire system was measured to be $0.660'$, which is much smaller than the level of tolerances. To predict the best focal position for the tilt measurement, we calculated the focal length of each lens set using ZEMAX. The post-assembly of the CQUEAN system after the lens assembly and alignment of the focal reducer were finished as shown in Fig. 8. The focal reducer was attached to the filter wheel through a specially designed adapter.

5. PERFORMANCE TEST

The engineering run of CQUEAN was carried out from 2010 August 10 to 17 at the 2.1 m Otto Struve telescope in McDonald Observatory, Texas, US. (See Park et al. (2012) and Kim et al. (2011) for the description of the engineering run). Fig. 9 shows the CQUEAN attached to the 2.1 m Otto Struve Telescope. During the run, operational tests of all components of CQUEAN including the camera and its optical component were carried out.

Filled with many stars throughout the FOV, a star cluster is an ideal target to inspect the image quality of an imaging instrument such as CQUEAN. A field in NGC 6633, an open cluster, was observed with each filter to investigate the optical performance of the focal reducer. The telescope focus was adjusted before the observations in each filter band, to investigate whether it varied according to wavelength bands. We confirmed the optimized distance between the primary and secondary mirrors for the best telescope focus at central wavelength of each filter. These values were calculated by ZEMAX program and listed in Table 6. For all bands except g and r, best focus was achieved at the same position. However, best i-band focus was obtained at slightly different position, and we had to adjust the focus significantly for g- and r-bands.

Fig. 10 shows the predicted and measured FWHM value against the radial distance from the image center. The FWHMs get larger at the outer region on g-, and r-band images due to coma aberration. These data are measured from actual images by SExtractor (Bertin & Arnouts 1996). Vignetting is seen in raw object images at all four corners of the image due to the limited diameters of focal reducer optics, although it can be reduced to some extent with flat fielding. Severe coma aberration is seen in the outer part of g-band image, and there is moderate coma aberration in r-band image as well. The aberration is caused by the focal reducer

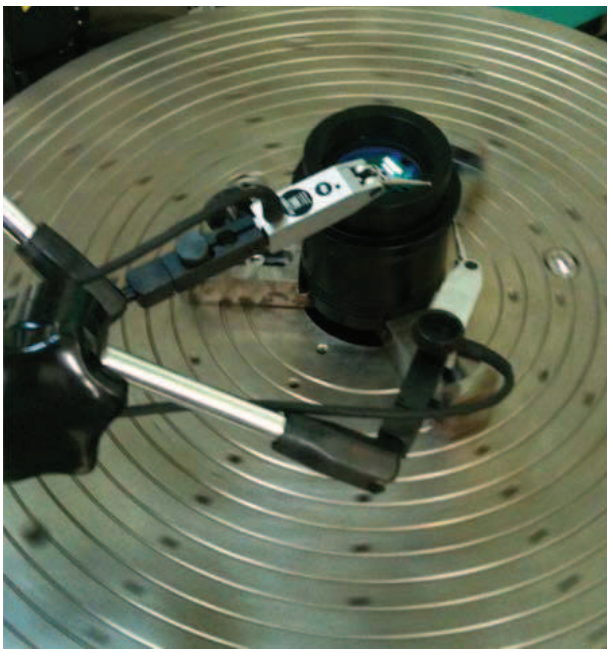

Fig. 7.— Alignment setup for the lens module of the focal reducer. Initial placement of the lens barrel is being measured by the probes on the testing plate.

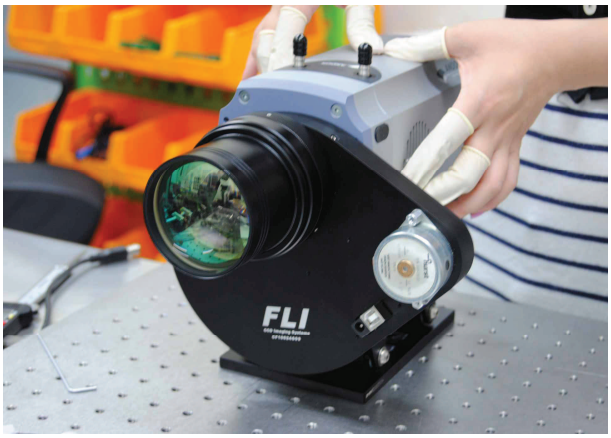

Fig. 8.— Post-assembly of the CQUEAN system, where the focal reducer and its outermost lens are shown as a cylindrical barrel in front of the FLI filter wheel.

Table 5.
Results from tilt measurements during the lens assembly. The lenses are installed in sequence from left (Lens 3) to right (Lenses 3, 2, 1). Predicted focal lengths are results from the ZEMAX calculation to find initial point for the measurement

Parameter	Lens 3	Lenses 3,2	Lenses 3,2,1
Radius of image rotation (mm)	0.070	0.077	0.042
Measured focal length (mm)	258.569	144.969	213.315
Predicted focal length (mm)	297.995	137.959	212.484
Tilt (arcmin)	0.936	1.800	0.660

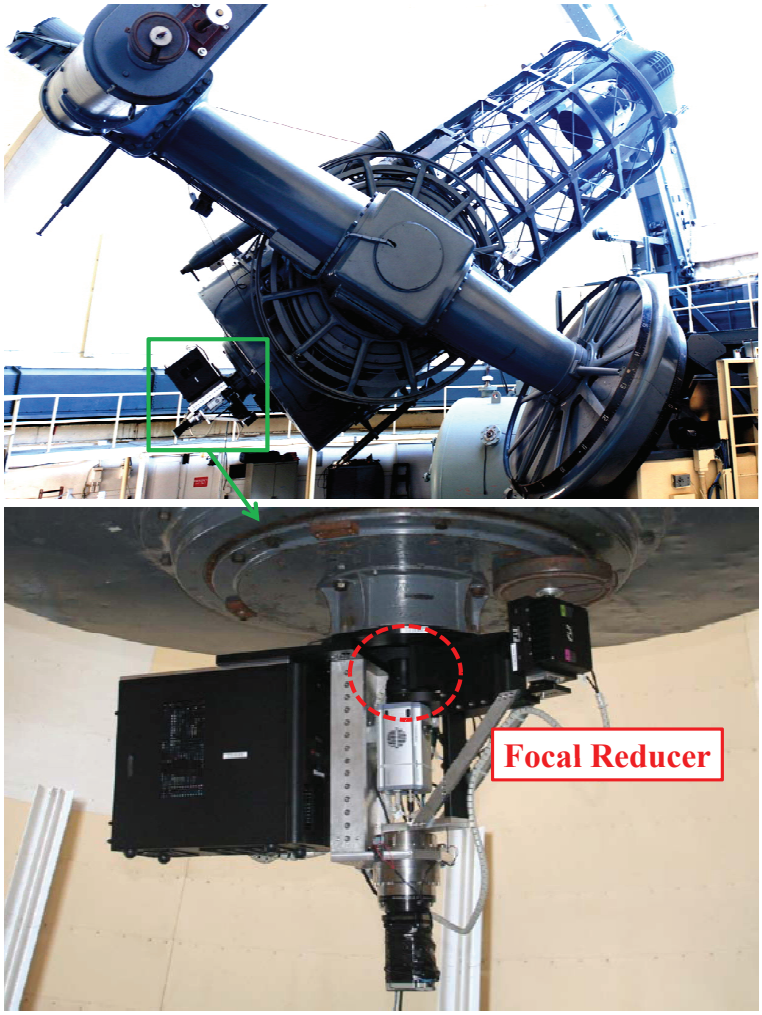

Fig. 9.— CQUEAN attached to the 2.1 m Otto Struve telescope. Science CCD camera is the silver box in the center, and guide CCD camera is the small black box in the upper right part of the system. The big black box in the left is the control PC. The motor below the science CCD camera moves the arm to rotate guide CCD camera (Kim et al. 2011). The location of the focal reducer is indicated in the bottom panel.

Table 6.
Optimized distance between two mirrors for the best telescope focus at each filter

Filter	Central wavelength (μm)	Telescope focus (distance between the primary and secondary; mm)
g	0.47	6079.89
r	0.62	6079.18
i	0.75	6079.04
z	0.88	6079.00
Y	1.01	6078.98

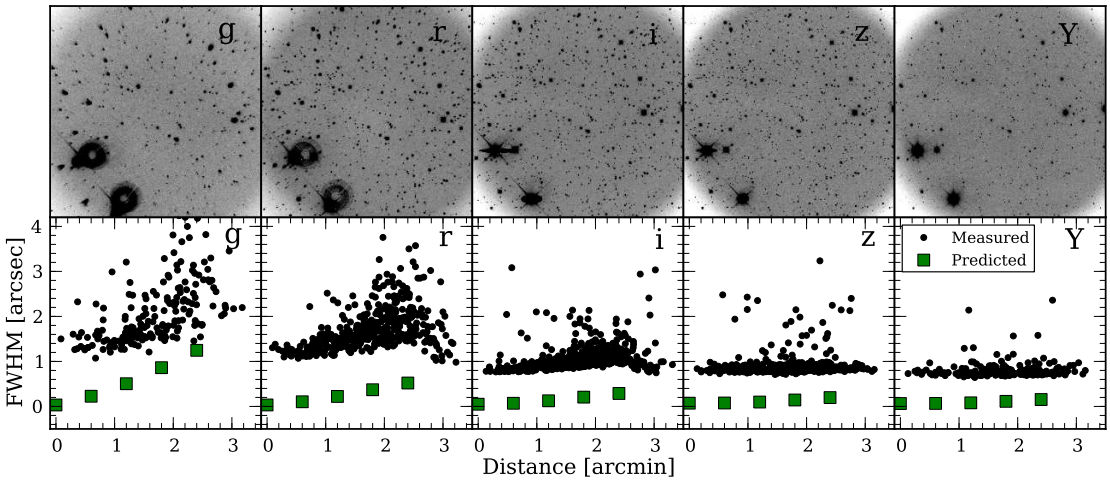

Fig. 10.— (Top) Raw images of open cluster NGC 6633 with CQUEAN. Each band was observed with 60 second exposure time, and focus was adjusted before observation of each band to ensure that all band images are in focus. (Bottom) FWHM vs. radial distance from the image center. The black circles are the observed data, and the green squares the predicted values from ZEMAX simulation. The differences between two data are caused by the non-ideal seeing condition.

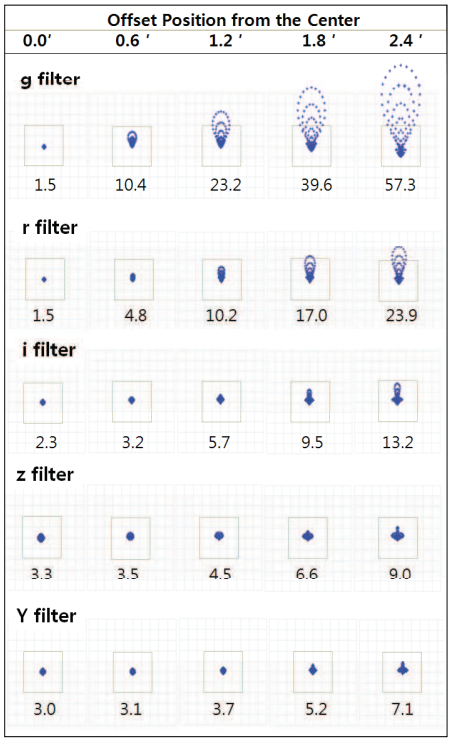

Fig. 11.— ZEMAX simulation of coma aberration on five filter bands of CQUEAN. Coma is quite large in g- and r-bands, but it gets smaller in wavelength bands longer than i-band, i.e., smaller than the size of single pixel. The figure represents the size and shape of each spot seen from the center to 2.4 minute position on the image plane. Values below spots are RMS size in the unit of μm.

since g-band and r-band were not considered as major bands for CQUEAN in the optical design of the focal reducer. However, little aberration was observed for other filter images.

This result is already expected from the ZEMAX simulation shown in Fig. 11. We considered five field points up to $2.4'$ from the on-axis by entering the center wavelength of each filter. ZEMAX simulation predicts that there is large coma at the edge position of g-band image and that the coma gets smaller on longer wavelength bands. For example, the RMS spot diameter at an edge position $2.4'$ away from the image center is predicted to be 57.3 μm on g-band, while only 7.054 μm on Y-band.

Each filter has a relatively narrow band width, so we are not concerned with chromatic aberration within a band. We tried to find the optimized telescope focus (position of the secondary mirror with respect to the primary mirror) for each filter as listed in Table 6. To get the best image (to minimize RMS spot size), the distance between the primary and secondary mirrors is used as a variable to optimize in the ZEMAX model while keeping the position of focal reducer constant. It turned out that focus adjustment is not necessary for five main bands (is, i, iz, z, Y) since it remains same within a 60 μm range, which is consistent with the result obtained from engineering run.

The degree of image degradation due to the coma aberration does not improve by adjusting the telescope focus. Therefore, for the g- and r-bands, we decided to abandon edges of the images and to use only the central region of the image plane.

6. CONCLUSION AND SUMMARY

The CQUEAN is an optical CCD camera optimized for the observation of high redshift quasars to understand the nature of early universe. The focal reducer was specifically designed to be used with the 2.1 m telescope of McDonald observatory and allows CQUEAN to secure a wider field of view by reducing the focal length of the telescope system by a factor of three. We designed the lens configuration, performed tolerance analysis, and estimated the optical performance with ZEMAX. Through an error analysis, which indicates how tilt, decenter, and despace of individual optical components affect the system performance, we found that our design of the focal reducer could meet all the requirements by CQUEAN. Then we designed opto-mechanical systems for the telescope hardware interface including the lens barrel.

We successfully attached the focal reducer and CQUEAN to the Cassegrain focus of the 2.1 m telescope at McDonald Observatory for a test run from August 10 to 17, 2010. Test images were obtained to verify the performance of the focal reducer. The test images are consistent the simulation result of ZEMAX.

ACKNOWLEDGMENTS

This work is supported by Creative Research Initiatives program of the Korea Science and Engineering Foundation (KOSEF), grant No. 2009-0063616, funded by the Ministry of Education, Science and Technology (MEST). Juhee Lim is partially supported by World Class University (WCU) program through the National Research Foundation of Korea funded by the MEST (R31-10016). The authors are indebted to Hyeonju Jeong, Eunbin Kim, Jinyoung Kim, Changsu Choi for encouragement and their assistance in obtaining the data at the McDonald Observatory, and Sungho Lee for careful proof readings of the manuscript. This paper includes data taken at The McDonald Observatory of The University of Texas at Austin.

REFERENCES

Bertin, E., & Arnouts, S. 1996, SExtractor: Software for Source Extraction, A&AS, 117, 393

Choi, C., Im, M., Jeon, Y., & Mansur, I. 2012, A Y-Band Look of the Sky with 1-m Class Telescopes, JKAS, 45, 7

Green, J. D., Robertson, P., Baek, G., et al. 2013, Variability at the Edge: Optical near/IR Rapid-Cadence Monitoring of Newly Outbursting FU Orionis Object HBC 722, ApJ, 764, 22

Kim, E., Park, W.-K., Jeong, H., et al. 2011, Auto-Guiding System for CQUEAN (Camera for Quasars in Early Universe), JKAS, 44, 115

Lee, I., Im, M., & Urata, Y. 2010, First Korean Observations of Gamma-Ray Burst Afterglows at Mt. Lemmon Optical Astronomy Observatory (LOAO), JKAS, 43, 95

Opal, C. B., & Booth, J. A. 1990, Focal Reducer/CCD Detector System for the McDonald 2.1 m Telescope, Proc. of the SPIE, 1235, 263

Park, W.-K., Pak, S., Im, M., et al. 2012, Camera for QUasars in EArly uNiverse (CQUEAN), PASP, 124, 839

Schroeder, D. J. 2000, Astronomical Optics (San Diego: Academic)

Smith, G. H. 1998, Practical Computer-Aided Lens Design (Richmond: Willmann-Bell)

Smith, W. J. 2000, Modern Optical Engineering - The Design of Optical Systems (New York: McGraw-Hill)

Smith, W. J. 2005, Modern Lens Design (New York: McGraw-Hill)

Thöne, C. C., de Ugarte Postigo, A., Fryer, C. L., et al. 2011, The Unusual γ-Ray Burst GRB 101225A from a Helium Star/Neutron Star Merger at Redshift 0.33, Nature, 480, 72

Wilson, R. N. 1996, Reflecting Telescope Optics 1 (Berlin: Springer)